Acta Cryst. (1965). **18**, 375

Translation-Permutation Operator Algebra for the Description of Crystal Structures. II. Interstice Lattice Stacking Faults*

By William G. Gehman and Stanley B. Austerman

Atomics International, a Division of North American Aviation, Inc., Canoga Park, California, U.S.A.

(*Received* 27 *February* 1964)

Interstice lattice stacking faults (ILSF) are predicted for *all* crystal structures that are composed of both (*a*) anion lattices that are ideally closest packed and (*b*) cation interstice lattices that are only *partially* occupied. For brevity, theoretical examples are given only for the ZnS, CdX_2, and spinel structures. Translation-permutation operator representations are presented for *basal* and *prismatic* ILSF which respectively lie perpendicular and parallel to the stacking axis, and for *pyramidal* ILSF which are tilted with respect to the *c* axis. Local charge unbalance occurs in both the basal and prismatic ILSF, and the basal ILSF also exhibits a local non-stoichiometry. Experimental examples of isolated ILSF in BeO bicrystals are presented.

1. Introduction

In part I (Gehman, 1963*a*, 1964) it was noted, in the discussion of the standard ionic crystal structures (Gehman, 1963*b*), that there existed a formal twofold choice of ways of writing the translation-permutation operator (TPO) formulae for the ZnS and the CdX_2 structure types (where X is a halide anion). The generalization approach of the TPO crystal algebra suggests the investigation of the result of combining these two ways of writing the TPO formulae for a given structure in only a single TPO formula, *i.e.* combining both forms of the crystal structure in one and the same crystal. This investigation leads to the concept of the type of crystal defect discussed in the present paper, namely a stacking fault that occurs entirely within the interstice lattice (as defined in part I, § 7) of an ideal closest packed atom lattice, and is thus termed an *interstice lattice stacking fault* (ILSF).

The generalization approach of the TPO crystal algebra also suggests that such defects are possible in *all* close-packed crystal structures in which either the octahedral or tetrahedral interstices, or both, are only *partially occupied*; *e.g.* complex structures such as carborundum-III, α-Al_2O_3, spinel, perovskite, *etc.*, as well as the standard ZnS and CdX_2 structures. However, for brevity, the discussion in the present paper is restricted to the ZnS and CdX_2 cases except for a brief mention of the spinel structure; the extensions to the more complex cases are straightforward.

Strock (1960) has suggested a defect which is equivalent to one of the special cases of basal ILSF presented below (equation (4)) in order to explain birefringence discontinuities in highly defective ZnS crystals; this specific suggestion was the outgrowth of earlier work on birefringence banding in which the idea behind basal ILSF in ZnS structures was qualitatively suggested (Strock, 1957; Strock, Brophy & Peters, 1958). The present concepts include and go beyond Strock's interpretations, and the present broader concepts do not appear to have been suggested before.

Most of the discussion in this paper will be based upon a hypothetical model consisting of an ideally closest-packed lattice of relatively large atoms (usually anions) that is completely free of classical stacking faults, the smaller atoms (usually cations) being distributed over the interstice lattice. Classical stacking faults can be distinguished from ILSF on two counts: (*a*) The former occur in the closest-packed lattice (and affect the interstice lattice by causing such defects as the electrostatic faults described by Kronberg, 1957); (*b*) the *atom displacement vector*, describing the generation of a stacking fault in an initially perfect crystal, has components only perpendicular to the *c* axis in the case of classical stacking faults, but also has non-zero components parallel to the *c* axis in the case of ILSF. Point defects and dislocations will be assumed to exist in the model and to compensate at least partially for local non-stoichiometry due to ILSF; beyond this, such defects will not be considered in this paper.

2. ZnS structures

The ZnS structure arises by the successive stacking of layers of closest-packed atoms and layers of tetrahedral interstitials in an alternating sequence. Because of the half-occupancy of the tetrahedral interstices by the cations, the TPO formula can be

* This work was carried out under the auspices of the United States Atomic Energy Commission, Contract Number AT-(11-1)-GEN-8. The paper was presented to the American Physical Society, Pasadena, December 1963.

Table 1. *TPO formulae for* ZnS *and* CdX_2 *basal ILSF structures*

ZnS structure:

$$(000)SY(100)\ldots Y(100)Y(100)Y(100)Y(100)\ldots Y(100)S(100) = \text{ideal}(1) \quad (1)$$

$$(001)SY(001)\ldots Y(001)Y(001)Y(001)Y(001)\ldots Y(001)S(000) = \text{ideal}(2) \quad (2)$$

$$(000)SY(100)\ldots Y(100)Y(100) \mid Y(001)Y(001)\ldots Y(001)S(000) = (+,-)\delta- \quad (3)$$

$$(001)SY(001)\ldots Y(001)Y(001) \mid Y(100)Y(100)\ldots Y(100)S(100) = (-,+)\delta+ \quad (4)$$

$$(000)SY(100)\ldots Y(100)Y(101)Y(001)\ldots Y(001)S(000) = (+,-)\delta+ \quad (5)$$

$$(001)SY(001)\ldots Y(001)Y(000)Y(100)\ldots Y(100)S(100) = (-,+)\delta- \quad (6)$$

CdX_2 structures:

$$\ldots Y(010)Y(000)Y(010)Y(000)\ldots = \text{ideal}(1) \quad (7)$$

$$\ldots Y(000)Y(010)Y(000)Y(010)\ldots = \text{ideal}(2) \quad (8)$$

$$\ldots Y(010)Y(000) \mid Y(000)Y(010)\ldots = \delta- \quad (9)$$

$$\ldots Y(000)Y(010) \mid Y(010)Y(000)\ldots = \delta+ \quad (10)$$

written in either of two ways. Using the definitions of part I, equation (1) in Table 1 corresponds to the exclusive occupancy of (+)-tet interstitial sites and equation (2) to the exclusive occupancy of (−)-tet sites, but the two ideal structures are physically equivalent since they are related by a horizontal reflection symmetry operation, σ_h. The surface TPO, S, are included in these equations to emphasize the surface effects of the crystal polarity of the ZnS structure (Gatos & Lavine, 1960; Warekois, Lavine, Mariano & Gatos, 1962): (1) exhibits an anionic bottom layer and a cationic top layer, and just the reverse holds for (2). Note that left-to-right in the TPO formulae corresponds to a bottom-to-top or a positive c direction in the crystals.

In the equations of Table 1 a structureless dummy symbol, Y, has been used for the unit TPO so as to ignore complications due to symmetry differences which arise when the Y symbols are replaced by R and L unit TPO in order to represent specific crystal structures. This step is taken to enhance clarity in the initial presentation of the ILSF concept. In actual practice, of course, the interaction of the real crystal symmetry with the ILSF is significant as discussed in § 4.

A single stacking error can occur in any one of four different ways, leading to the four types of *basal* ILSF listed in equations (3) through (6) in Table 1; the adjective 'basal' indicates that these ILSF twin planes lie parallel to the closest-packed planes. It is assumed that the crystal is constructed in a *layer-by-layer* fashion, starting with the bottom layer, in a direction parallel to the stacking axis which is [111] in c.c.p. and [0001] in h.c.p. Then the general viewpoint to keep in mind is that: (*a*) the construction of structures (3) through (6) has been started according to one of the two *ideal* fashions represented by either equation (1) or (2); (*b*) but that at one intermediate step an error was made in the stacking of an entire cation layer; and (*c*) that above this basal stacking fault the crystal construction continued according to the alternate ideal structure, *i.e.* either equation (2) or equation (1) respectively.

A number of comments are in order concerning equations (3) through (6). The center of the ILSF is indicated by a vertical line in Table 1, and corresponds to a twin plane in the sense defined by Cahn (1954). In equations (3) and (4), the twin plane due to the ILSF coincides with the mid plane of a closest-packed monolayer, but in equations (5) and (6) the twin plane is halfway between two adjacent monolayers and lies in the plane of the octahedral interstices. In equations (4) and (5), the nearest neighbor planes of occupied tetrahedral interstices on each side of the twin plane are separated by a distance $t_c/2$ parallel to the c axis, but they are separated by $3t_c/2$ in equations (3) and (6), where t_c, the unit of length along the c-coordinate axis, is the distance between adjacent, parallel planes of ideally closest-packed atoms. Thus the twin plane experiences a higher-than-normal positive charge in equations (4) and (5), and a higher-than-normal negative charge in equations (3) and (6); these two types of ILSF will be defined as '$\delta+$' and '$\delta-$' types respectively. The order in which the tetrahedral interstices are met as one proceeds in a positive c direction is also a distinguishing characteristic and will be denoted by $(+,-)$ and $(-,+)$ as the case may be. Thus the long left-hand sides of equations (3) through (6) can be succinctly summarized as shown on the right-hand sides of those equations.

It should be noted that the stoichiometry of the crystal is upset in the region of the ILSF, and also the local charge balance as described above. It is assumed that point defects, dislocations, and the set of normally empty tetrahedral interstices act as sinks for the cations from the missing plane. A corollary of this assumption is that the local non-stoichiometry

is not communicated to the surface of the crystal and this appears to be borne out by the experimental observations reported below.

3. CdX_2 structures

Only half as many types of basal ILSF occur in the CdX_2 structures as occur in the ZnS structures since there is only one set of octahedral interstices compared with the two sets of tetrahedral interstices. Equations (7) and (8) represent the two possible ideal structures which are related by a σ_h symmetry operation. Ellipses, ..., are used to indicate infinite crystals. The crystal surface is ignored because the CdX_2 structure does not exhibit a crystal polarity, nor the attendant surface effects, since the octahedral interstices are symmetrically spaced halfway between the closest packed monolayers. Equations (9) and (10) represent the two types of basal ILSF in the CdX_2 structures.

4. Effect of crystal symmetry upon ILSF interfacial energies

Caution must be exercised in using the structureless dummy symbols, Y, of Table 1 since the interfacial energies of ILSF, and hence their relative probabilities of occurrence, can depend upon the symmetry of the crystal structure, *i.e.* upon the sequence of R and L unit TPO in the TPO structure formula. In ZnS structures, ILSF (3), (6), and (5) are relatively insensitive to the crystal structure since: (*a*) in (3) and (6) the cation–cation layers across the ILSF twin plane are separated by a relatively large distance, $3t_c/2$; and (*b*) in (5) the relative disposition of the two layers of tetrahedral interstices within a single closest packed double layer is independent of its being R or L. However, the $(-, +)\delta+$ ILSF of equation (4) is strongly affected according as it occurs within an $RR=LL=$ cubic triple layer, or within an $RL=LR=$ hexagonal triple layer, since the interatomic separation of nearest neighbor cation–cation atom pairs differs in the two cases. In the RR case, this cation–cation separation distance has components normal to as well as parallel to the c axis, and thus has a magnitude of $\sqrt{2}.r_{cp}$, where r_{cp} is the radius of a closest packed sphere. But in the RL case, the a_1- and a_2-components are zero and the nearest neighbor cations are now only separated by a distance $t_c/2=\sqrt{\frac{2}{3}}.r_{cp}$. Thus the RL form of (4) has a much higher repulsive energy than the RR form, in accord with electrostatic energy calculations (Gehman, 1965). One can therefore infer that, if such an ILSF occurred in a hexagonal wurtzite structure, it would be favorable to have a classical stacking fault coincide with the ILSF so as to convert the RL triple layer into an RR form.

In the CdX_2 structures, the $\delta-$ ILSF of equation (9) is relatively insensitive to the nature of the triple layer in which the ILSF occurs, since the nearest-neighbor cation layers across the ILSF are separated by a distance $3t_c$. However, the $\delta+$ ILSF of equation (10) is sensitive to the crystal structure in which it occurs. This ILSF is equivalent to a thin layer of either an NaCl or an NiAs structure within the CdX_2 structure with the cation layers separated by a distance t_c, and it has been shown (Zemann, 1958) that hexagonal NiAs is electrostatically less stable than cubic NaCl. Thus, a $\delta+$ ILSF in hexagonal CdI_2 would be less stable than one in cubic $CdCl_2$, and in the former case, the coincidence of a classical stacking fault with the $\delta+$ ILSF would lower the energy and make the defect less unstable.

5. Multiple TPO; partial ILSF; prismatic ILSF;

Sets of more than one type of TPO, or *multiple* TPO, were required for the representation of point defects in part I (§ 12). Multiple TPO also permit the description of polycrystalline materials. The simplest case (to which this paper will be mainly limited) arises with the use of only two parallel TPO to represent a bicrystal which has its dividing interface parallel to the c axis. In the present ILSF context the further restriction holds that the anion layers are continuous and perfectly closest packed right across the dividing boundary.

The effect of combining, for example, equations (1) and (3) is diagrammatically illustrated in Fig. 1(*a*), where the solid lines represent the closest-packed anion mid planes and the dashed, horizontal lines represent the mid planes of either the (+)-tet or (−)-tet layers which are *actually occupied by cations.* It is seen that two types of ILSF occur in this case. First there is a basal ILSF of type (3) that extends only part way across the crystal and is thus termed a *partial* $(+, -)\delta-$ basal ILSF; this partial basal ILSF is indicated by the heavy solid lines. Second there is another partial ILSF where the twin plane lies parallel to the c axis and hence parallel to the prismatic planes in h.c.p.; this type is termed a partial *prismatic* ILSF, and is indicated by the dotted line. A fault will be termed a *pyramidal* ILSF if its macroscopic twin boundary is neither perpendicular nor parallel to the c-axis as in the basal and prismatic cases respectively.

In the present paper, the atomic features along the dotted line in Fig. 1 will not be considered for the different possible sequences of multiple TPO and partial ILSF. However, one microscopic detail will be emphasized since it is common to all possible types of prismatic and pyramidal ILSF, and this is the step discontinuity that occurs in the occupancy of the interstice layers. Only the ZnS structure type will be discussed, and here the step discontinuity occurs between the layers of tetrahedral interstices with c coordinates $c=n+\frac{1}{4}$ and $c=n+\frac{3}{4}$ within a closest packed double layer with monolayer mid-

planes at $c=n$, $n+1$ (n an integer). This is illustrated in a top view in Fig. 2 where the upper monolayer at $c=n+1$ has been removed to expose the lower closest packed monolayer at $c=n$ and the intervening partially occupied tetrahedral interstice layers. The tetrahedral interstitials at $c=n+\frac{1}{4}$ are shown as small open circles and those at $c=n+\frac{3}{4}$ as small solid circles; in addition, the one-to-one stoichiometry has been maintained by arbitrarily locating the small open circles on lattice points of the form $((m+\frac{2}{3}), (n+\frac{1}{3}), \frac{1}{4})$ in (a_1, a_2, c) coordinates with the origin at the center of a closest packed anion, m and n being integers. The intersection of a prismatic ILSF, of the type illustrated in Fig. 1(*a*), with a basal anion layer has been quite arbitrarily drawn in Fig. 2 so as to lie in two first order and one second order h.c.p. prism planes, as indicated by the intersection directions [100], [0$\bar{1}$0], and [$\bar{2}\bar{1}$0] respectively.

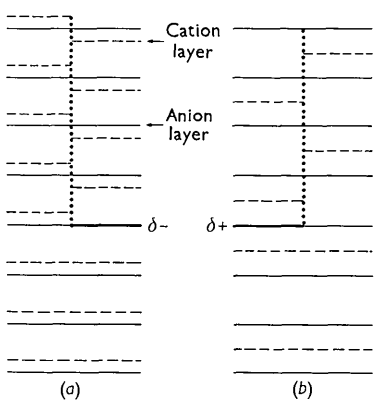

Fig. 1. Diagrammatic representation of partial basal ILSF (heavy horizontal lines) and partial prismatic ILSF (dotted vertical lines). (*a*) ZnS structure type. (*b*) CdX_2 structure type.

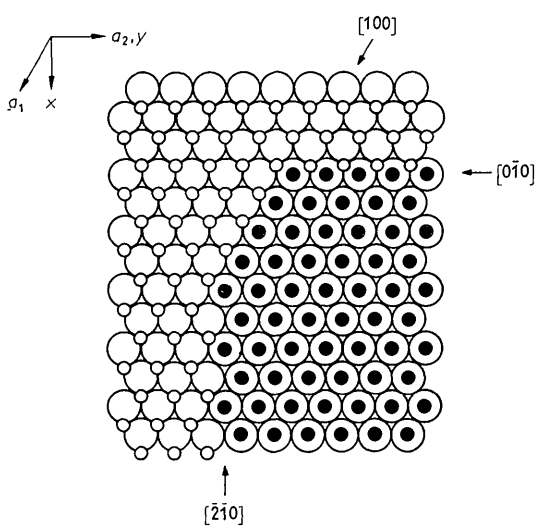

Fig. 2. Example of a step discontinuity in the occupancy of the tetrahedral interstice layers in ZnS type structures containing prismatic ILSF. Large open circles: anions with c coordinate $c=n$ (n an integer). Small open circles: cations at $c=n+\frac{1}{4}$. Filled circles: cations at $c=n+\frac{3}{4}$.

An important feature of this step discontinuity is illustrated in Fig. 2, namely, that an *electrostatic mismatch* necessarily occurs, compared to the ideal structure as a reference point, owing to a change in the coordination number of the ions along the ILSF boundary. Thus along the [0$\bar{1}$0] and [100] boundaries in Fig. 2 the cations within a single closest-packed double layer are separated by a nearest neighbor distance of $\sqrt{2}.r_{cp}$ which is less than the ideal nearest neighbor separation of $2r_{cp}$. Thus both of these boundaries would have a greater electrostatic repulsive energy than the ideal crystal; the [0$\bar{1}$0] boundary has a higher repulsive energy than the [100] boundary since there are twice as many interactions of the same magnitude. The [$\bar{2}\bar{1}$0] boundary as drawn in Fig. 2 has distances of magnitude $\sqrt{2}.r_{cp}$ (but fewer in number than in the former two cases) plus distances of length $\sqrt{6}.r_{cp}$ which is greater than the ideal crystal; thus the energy of this boundary should be roughly comparable to the ideal case. The cation–cation repulsive electrostatic energy can be either greater or less than the ideal case, depending upon the location of the small open circles in Fig. 2; alternative cases to those shown in that figure can be found by locating these circles on lattice points of the form $((m-\frac{2}{3}), (n-\frac{1}{3}), \frac{1}{4})$. But in *all* cases, an electrostatic mismatch arises which might be expected to perturb the positions of the atoms in the neighborhood of prismatic or pyramidal ILSF in order to lower the crystal energy, somewhat analogous to the atom shifts in α-Al_2O_3 (Kronberg, 1957), and thus lead to a strained region in the crystal. Evidence of just such a strained region has been found in BeO by Austerman & Newkirk (1963) by X-ray diffraction topography.

The discussion of this section can be extended to the CdX_2 case. A hypothetical example of a partial basal ILSF plus a partial prismatic ILSF in such a structure, formed by combining TPO (10) and (8), is illustrated in Fig. 1(*b*). In this case the discontinuity of the occupancy of the cations in the partial prismatic ILSF occurs within an anion triple layer, with the complete layer of octahedral interstices being made up of two parts, one in the lower anion double layer and one in the upper double layer of the overall triple layer.

6. Spinel ILSF

As an example of the extension of the ILSF concept to more complex structures, basal ILSF in the spinel structure will be briefly mentioned. Equations (11) and (12) in Table 2 represent two ways of writing the TPO formula for ideal spinel (see part I, § 10). The difference between the two is most readily seen by comparing permutation pseudovector IV in the two cases; these two pseudovectors have been shifted

Table 2. *TPO formulae for basal ILSF in the spinel structure*

I	$\ldots R(001)R(000)R(100)R(010)R(010)R(010)\ldots$		
II	$\ldots R(100)R(010)R(010)R(010)R(001)R(000)\ldots$	= ideal(1)	(11)
III	$\ldots R(010)R(010)R(001)R(000)R(100)R(010)\ldots$		
IV	$\ldots R(000)R(010)R(000)R(010)R(000)R(010)\ldots$		
I	$\ldots R(000)R(100)R(010)R(010)R(010)R(001)\ldots$		
II	$\ldots R(010)R(010)R(010)R(001)R(000)R(100)\ldots$	= ideal(2)	(12)
III	$\ldots R(010)R(001)R(000)R(100)R(010)R(010)\ldots$		
IV	$\ldots R(010)R(000)R(010)R(000)R(010)R(000)\ldots$		
I	$\ldots R(001)R(000)R(100) \mid R(010)R(010)R(001)\ldots$		
II	$\ldots R(100)R(010)R(010) \mid R(001)R(000)R(100)\ldots$	= xs tet	(13)
III	$\ldots R(010)R(010)R(001) \mid R(100)R(010)R(010)\ldots$		
IV	$\ldots R(000)R(010)R(000) \mid R(000)R(010)R(000)\ldots$		
I	$\ldots R(000)R(100)R(010) \mid R(010)R(010)R(010)\ldots$		
II	$\ldots R(010)R(010)R(010) \mid R(010)R(001)R(000)\ldots$	= xs oct	(14)
III	$\ldots R(010)R(001)R(000) \mid R(000)R(100)R(010)\ldots$		
IV	$\ldots R(010)R(000)\underline{R(010) \mid R(010)}R(000)R(010)\ldots$		

relative to one another in the identical fashion as equations (7) and (8) for the CdX_2 case. Then starting with (11) and passing to (12) leads to the basal ILSF TPO of equation (13), and reversing the process leads to that of (14). The names of these two ILSF are derived by focusing attention upon the closest-packed triple layer (indicated by the brace) that is split by the ILSF twin plane. In the ideal structure this pair of double layers contains 4 octahedral and 2 tetrahedral interstices. But in (13) there are 2 octahedral plus 4 tetrahedral or an excess of tetrahedral interstices compared with the ideal structure, hence the name 'xs tet'. And in (14) there are 6 octahedral and 0 tetrahedral or an excess of octahedral interstices, hence the name 'xs oct'. The ILSF are not designated in terms of electrostatic charge since this varies widely with the type of spinel and whether it is inverse or normal.

7. Experimental observations of ILSF

The discussion of interstice lattice stacking faults to this point has been largely conceptual in character. It is quite possible that not all the structures described will be found in nature. However, some of the structures are known to exist in real crystals, and very likely other examples will be found.

Strock and coworkers have studied polytype structures in ZnS crystals in great detail (Strock & Brophy, 1956; Buck & Strock, 1956; Strock, 1957; Strock, Brophy & Peters, 1958). These highly defective ZnS crystals characteristically exhibit birefringence banding in which bands with distinct values of birefringence meet at sharp boundaries. These boundaries have been qualitatively interpreted in terms closely parallel to the present basal ILSF concept (Strock, 1957; Strock, Brophy & Peters, 1958) and, in fact, Strock (1960) specifically inferred the existence of a stacking defect that is equivalent to basal ILSF (4). Unfortunately, none of these experimental examples exhibited isolated unambiguous ILSF; other types of defect complicated the structure so that the presence of the ILSF was not obvious but could only be inferred from X-ray and birefringence studies.

Striking examples of apparently isolated ILSF are found in the BeO bicrystals grown by Austerman (1962). The BeO structure is of the ZnS type (*B*4, wurtzite) which exhibits a crystal polarity due to the asymmetric location of the cations between the anion layers (see equations (1) and (2)). The ILSF in this structure lead to the formation of *inversion twins*, so called because the crystal regions on each side of the twin boundary, or the stacking fault boundary, have opposite or inverted crystal polarities. The inversion twins are most evident in the morphology of crystals grown from solution in lithium molybdate (Austerman, 1963). Photographs of BeO bicrystals containing ILSF are shown in Figs. 3, 4, and 5.

Fig. 3 shows an inversion twin with a basal ILSF twin plane parallel to the basal planes of the crystal. From morphology and from etching experiments (Austerman, Berlincourt & Krueger, 1963), it is believed that the large opposing end faces are oxygen-rich $(000\bar{1})$ faces, and hence the crystal corresponds to either equation (3) or (5) in Table 1.

Fig. 4 shows a top view of an inversion twin platelet crystal with a $(11\bar{2}0)$ prismatic ILSF twin boundary. The presence of etch patterns on only one side of the boundary, and their absence on the other side, clearly exhibits the opposite crystal polarities of the two regions of the bicrystal.

Fig. 5 shows an interesting and quite prevalent case in which an inner region or *core* of one crystal polarity is surrounded by an outer region of opposite crystal polarity. The fault is a pyramidal ILSF since the twin boundary is tilted with respect to the *c* axis. However, the degree of tilt in this type of cored crystal is typically very slight (often less than one degree), thus these ILSF do not differ very much from the prismatic case. In addition to these examples of isolated types of ILSF, examples have also been

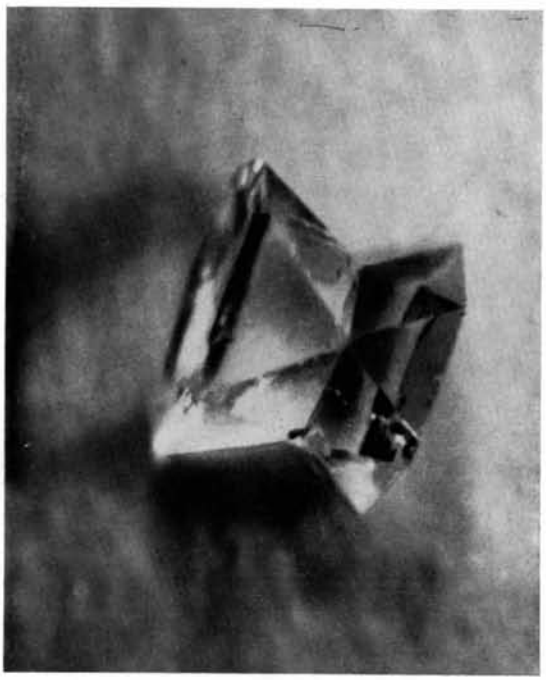

Fig. 3. BeO 'dumbbell' bicrystal with a basal ILSF twin plane.

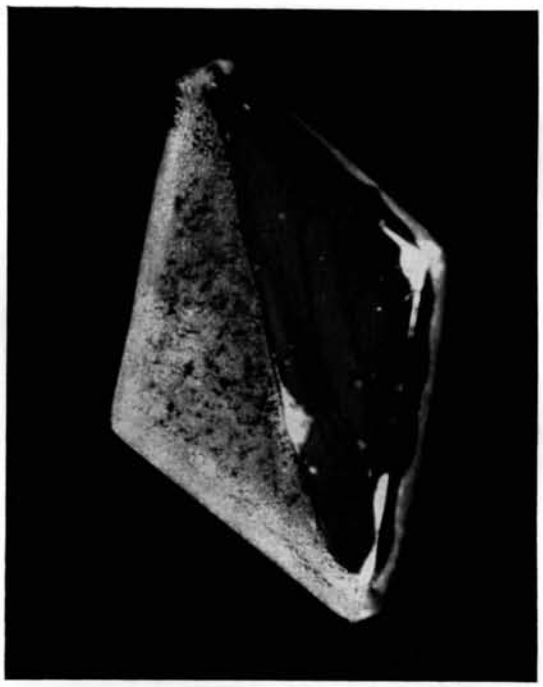

Fig. 4. BeO platelet bicrystal with a prismatic ILSF twin plane.

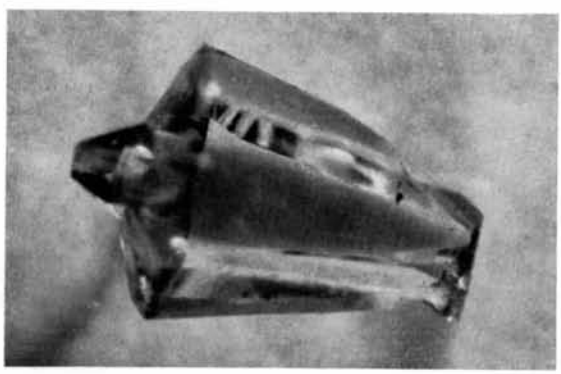

Fig. 5. BeO 'cored' bicrystal with pyramidal ILSF twin planes.

[*To face p.* 379

found in which basal and cored twinning occurred simultaneously in a given BeO polycrystal.

The occurrence of inversion twinning has been observed also in polycrystalline BeO (Rau, 1962). In this case, electron microscopy of replicas taken from polished and etched samples sometimes revealed regions of etching and of non-etching in the cross-section of a given grain. This was interpreted, probably correctly so, as due to inversion twinning within the grain.

The reported examples of ILSF are both in polar crystals, ZnS and BeO. To the authors' knowledge, there have been no reports of (*a*) ILSF in polar structures other than ZnS and BeO, (*b*) ILSF in CdX_2 structures, or (*c*) ILSF in more complex structures such as spinel, *etc.* This might well be due to the fact that the observable experimental effects of ILSF in these crystals might be quite small in other than certain specialized physical measurements. However, the presence of ILSF in such crystals should certainly be looked for.

It should be noted that in the observed cases in real crystals, there may be other defects associated with the ILSF. Although it is beyond the scope of the present paper to discuss the other defects, it should be realized that in real crystals classical stacking faults, impurity concentrations, dislocations, *etc.* might be associated with the ILSF, helping to reduce the overall energy of the system.

8. Conclusions

The generalized concept of a new class of lattice defects, interstice lattice stacking faults, or ILSF, has been enunciated in terms of the TPO crystal algebra. Three main types of ILSF are postulated and experimental evidence for their existence presented: basal and prismatic ILSF which respectively lie perpendicular and parallel to the *c* axis, and pyramidal ILSF which are tilted with respect to the *c* axis. The ILSF may have local regions of charge unbalance and non-stoichiometry connected with them. Although only limited experimental evidence of ILSF has been reported to date, ILSF should, in principle, occur in a wide variety of crystals which have partially occupied interstice lattices.

References

Austerman, S. B. (1962). Atomics International report NAA–SR–6425.

Austerman, S. B. (1963). *J. Amer. Ceram. Soc.* **46**, 6.

Austerman, S. B., Berlincourt, D. A. & Kreuger, H. H. A. (1963). *J. Appl. Phys.* **34**, 339.

Austerman, S. B. & Newkirk, J. B. (1963). Private communication.

Buck, D. C. & Strock, L. W. (1956). *Amer. Min.* **40**, 192.

Cahn, R. W. (1954). *Advanc. Phys*, **3**. 363 (esp. p. 368.)

Gatos, H. C. & Lavine, M. C. (1960). *J. Electrochem. Soc.* **107**, 427.

Gehman, W. G. (1963*a*). Atomics International report NAA–SR–8377.

Gehman, W. G. (1963*b*). *J. Chem. Educ.* **40**, 54.

Gehman, W. G. (1964). *Acta Cryst.* **17**, 1561.

Gehman, W. G. (1965). Publication in preparation.

Kronberg, M. L. (1957). *Acta Metallurg.* **5**, 507.

Rau, R. C. (1963). *J. Amer. Ceram. Soc.* **46**, 484.

Strock, L. W. & Brophy, V. A. (1956). *Amer. Min.* **40**, 94.

Strock, L. W. (1957). *Acta Cryst.* **10**, 840.

Strock, L. W., Brophy, V. A. & Peters, T. E. (1958). Electrochem. Soc. Meeting, New York: April.

Strock, L. W. (1960). *Illuminating Engineering*, **55**, 24.

Warekois, E. P., Lavine, M. C., Mariano, A. N. & Gatos, H. C. (1962). *J. Appl. Phys.* **33**, 690.

Zemann, J. (1958). *Acta Cryst.* **11**, 55.